Indoor monitoring system based on ARQ signaling generated by a Visible Light Communication link

Joan Bas*, Jose Antonio Ortega †, Martí Busquets†, and Alexis A. Dowhuszko‡
*Centre Tecnológic de Telecomunicacions de Catalunya (CTTC/CERCA), 08860 Castelldefels, Spain
†Universitat Politècnica de Catalunya (UPC), 08034 Barcelona, Spain
‡Department of Communications and Networking, Aalto University, 02150 Espoo, Finland
Email: joan.bas@cttc.es; {jose.antonio.ortega,marti.busquets}@estudiantat.upc.edu; alexis.dowhuszko@aalto.fi

***Abstract*—Visible Light Communications (VLC) is a candidate technology that complements the benefits of radio communication networks, particularly in those situations where a low-cost solution using license-free spectrum is required to enable ultra-dense deployments of indoor small cells. However, the main drawback that VLC has when compared to wireless communications on RF bands is that, in presence of obstacles between the transmitter and the receiver, full-blockage events are likely to happen as the power received on reflections is much weaker than the power of the blocked line-of-sight link. In this paper, we take advantage of this phenomenon and study the effect that different activities performed by people in the service area to-be-monitored have on the Automatic Repeat reQuest (ARQ) signaling of the VLC link. Based on the presented experimental studies, it is possible to conclude that different relevant events are able to be detected correctly according to the statistics of the ARQ signaling that is collected from the ongoing VLC transmission.**

***Index Terms*—Visible Light Communications; Automatic Repeat reQuest; Indoor sensing; Activity recognition; Software-defined demonstrator; Line-of-sight blockage.**

I. Introduction

Visible Light Communication (VLC) systems encode data into fast changes of the intensity of a visible light source, which are imperceptible to the human eye. Unlike conventional Radio Frequency (RF)-based wireless systems that require advanced digital signal processing, particularly when using Millimeter-Wave (5G) and Tera-Hertz (6G) RF bands [1], a VLC system utilizes low-cost, mass-produced, energy-efficient LEDs as transmitters [2]. At the receiver side, a VLC system relies on a Photodetector (PD) that senses the changes on the intensity of the *light signal* to estimate the data symbols that were transmitted. Apart from data communication and illumination services [3], VLC technology can be also used to monitor the status of the indoor environment by sensing the effect that people create on the received optical signal [4].

Nowadays, there is a wide range of technologies that can be used to monitor indoor environments. Apart from well-known camera based-surveillance systems and infrared sensors, there are also RF-based solutions that take advantage of the ubiquitous availability of Wi-Fi and 4G/5G nodes to sense the variations that the RF signals experience during propagation [5]. Most of these RF-based solutions require a wireless-enabled device on the target object to perform *active* monitoring, but there are also radio communication systems that carry out a *passive* sensing of the effect that moving obstacles (like people) create on the Received Signal Strength Indicator (RSSI) and/or Channel State Information (CSI) of an ongoing wireless data transmission [6], [7]. We note that both RSSI and CSI signaling belong to the PHY-layer of the wireless communication standard and that, so far, no passive monitoring solution has studied in detail the effect that people's activities create on the Data Link-layer signaling of an active link (*e.g.*, ARQ signaling messages and time-outs).

Automatic Repeat reQuest (ARQ) is an error control mechanism that wireless communication systems use to ensure the delivery of packetized data in the correct sequence. In an ARQ scheme, Cyclic Redundancy Check (CRC) is used to detect whether the received packet is in error or not. Therefore, when the Signal-to-Noise-plus-Interference power Ratio (SNIR) of the wireless link falls below the sensitivity threshold of the mobile terminal, the payload of the received packet becomes likely corrupted (even after forward error correction). In this situation, a Negative Acknowledgment (NACK) is fed back to the transmitter, and the re-transmission of the wrongly received packet is scheduled. If the transmitter does not receive a positive Acknowledgement (ACK) before the *time-out* timer expires, the packet is also re-transmitted [8]. ARQ is used by the MAC protocol of Wi-Fi to detect collisions in the contention-based (shared) radio channel, and can be combined with forward error correction of variable code rates to maximize the likelihood of reliable communication when multiple re-transmissions are triggered due to deep fading and/or strong interference [9]. Note that when the frequency of the wireless carrier moves beyond RF bands into VLC bands, the presence of full-blockage events become more likely, and the ARQ signaling can be used for indoor monitoring purposes.

In this paper, we study the effect that different people's activities create on the ARQ signaling of an ongoing VLC data link. In the experimental setting, a Phosphor Converted LED and a silicon PIN-based PD were used in the VLC transmitter and receiver, respectively. Both LED and PD were pointing to a large white wall, resembling the indirect illumination scenario presented in [10]. When people passed by the (direct) LED-wall link and (indirect) wall-PD link at different paces, a different pattern of ARQ signaling (*i.e.*, ACKs, NACKs, and

This work received funding from the Catalan Government under Grants 2017-SGR-00891 and 2017-SGR-01479, and the Spanish ministry of science and innovation under project IRENE PID2020-115323RB-C31 (AEI/FEDER,UE), and is based upon work from COST Action CA19111 NEWFOCUS, supported by COST (European Cooperation in Science & Tech.)

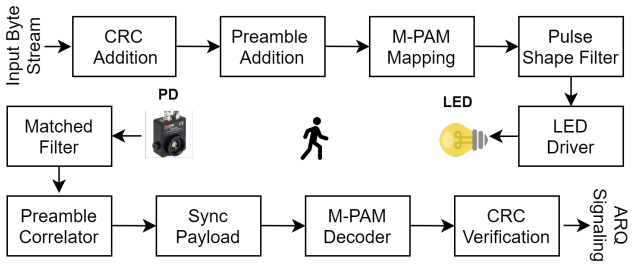

Fig. 1: Overview of the VLC link based on single-carrier M-PAM symbols and a Stop-and-Wait ARQ scheme. The statistics of the ACKs, NACKs, and time-out events in the transmitter are used to identify the presence of people carrying out different activities.

time-outs) was generated. These representative ARQ signaling patterns were studied in detail for different situations, showing notable variations that pave the way for using this information to train neural networks for machine learning classification.

The rest of this paper is organized as follows: Section II explains the software-defined VLC system that was implemented, whereas Section III provides the details of the ARQ signaling scheme and the geometry of the different people's activity situations that we aim to recognize. Section IV explains the demonstration setting and carries out the analysis of the ARQ signaling that was collected on the different experiments. Finally, conclusions are drawn in Section V.

II. Implementation Details of the VLC Link

The block diagram of the software-defined VLC link that was implemented to collect the ARQ signaling is shown in Fig. 1. It consists of a software-defined single-carrier M-PAM transmitter that generates a real-valued baseband signal, one LED driver that adapts the output voltage of the USRP to the input current of an LED array with 7 LUXEON Rebel Plus LXML-PWC1-0100 (cool-white) LEDs [11], and a Thorlabs PDA100A2 detector with switchable gain Transimpedance Amplifier (TIA) [12] that interfaces the (weak) current coming from the silicon PIN diode to the input voltage that the USRP needs to obtain the received signal samples.

A. Signal processing in the VLC transmitter and receiver

The VLC transmitter divides the input byte stream into payload packets of length L_{pl} bytes. After that, a known preamble sequence of length L_{p} bytes is added at the beginning, and CRC of length L_{crc} bytes is computed (based on the payload bytes) and appended after the payload. Finally, a guard band of L_{g} bytes is also added at the end of the packet to guarantee a minimum separation between consecutive packets (see Fig. 2).

The bytes of each VLC packet are divided into symbols and, after that, each of them are first mapped into points of an M-PAM constellation. Then, samples are pulse-shaped using a Square-Root Raised-Cosine (SRRC) filter. Finally, the signal is sent to the LED driver, which interfaces the output voltage of the USRP to the electric current that is needed to control accordingly the intensity of the light emitted by the LEDs.

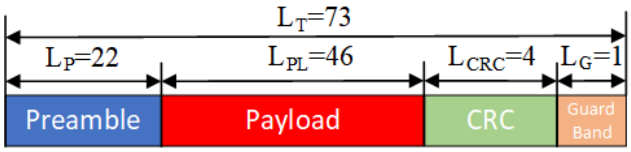

Fig. 2: Overview of the frame structure implemented in the software-defined VLC system that relies on ARQ signaling to monitor the indoor environment. The length of the frame fields are in bytes.

The optical signal that reaches the sensitive area of the PD generates a current that, after being amplified by the TIA, is sampled at a regular sampling time T_{s}. These signal samples go first through a SRRC matched-filter with the same roll-off factor used in the pulse-shaping filter of the VLC transmitter. Afterwards, the energy of the received signal samples is computed to identify whether there is an ongoing transmission or not, due to the bursty data traffic pattern that an ARQ scheme generates in the PHY-layer. Therefore, when the energy of the received signal samples is higher than a predefined threshold, the most likely position of the preamble is estimated from the sequence of received samples. After the position of the preamble is detected and the received signal samples that correspond to the payload-plus-CRC of the VLC frame are demodulated. Finally, the CRC for the received payload bytes is computed and compared with the received CRC bytes, to check whether the received packet is corrupted or not. Note that when implementing an ARQ scheme, the outcome of this CRC verification process is used to issue ACKs (or NACKs) to inform to the transmitter that the current data packet was properly received (or not).

B. Modelling the elements of the VLC channel

An LED is composed of a PN junction which, after the application of a forward voltage, experiences a reduction on the potential barrier of the junction, such that the movement of injected minority carriers (*i.e.*, electrons and holes) is induced. This movement results in electron-hole recombination events that emit photons on different wavelengths, which are centered at different *colors* according to the specific semiconductor materials that are used to manufacture the LED chip.

There are different LED technologies that could be used to generate white light with various Correlated Color Temperatures (CCTs) and suitable illuminance (or luxes) for different indoor environments. Without loss of generality, we consider the Phosphor-Converted (PC) white LED technology due to the low-cost, implementation simplicity, and good ability to render colors accurately [10]; however, the same approach can be applied to color LEDs. As shown in Fig. 3 a), a PC-LED consists of a Blue-Chip and a Yellow-phosphor layer, whose interaction generates white light with a CCT that depends on the balance between the emitted blue and yellow light [3].

To model the electrical response of an LED, it is necessary to find an equivalent DC model of the Shockley equation, *i.e.*,

$$I_{\mathrm{d}} = I_{\mathrm{s}} \left[\exp\left(V_{\mathrm{d}}/(N\, V_{\mathrm{t}})\right) - 1 \right], \tag{1}$$

where V_{d} is the voltage on the PN junction, N is the parameter known as the emission coefficient, $V_{\mathrm{t}} = 25.8\,\mathrm{mV}$ is the typical

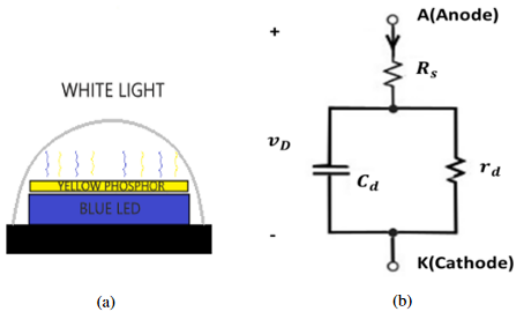

Fig. 3: a) The CCT of the white light emitted by a PC-LED depends on the photons coming from the Blue Chip and Yellow-phosphor layer. b) Equivalent small-signal circuit of a commercial LED used to model its frequency response. Here, R_s, C_d, and r_d are the series resistance, diffusion capacitance, and diffusion resistance, respectively.

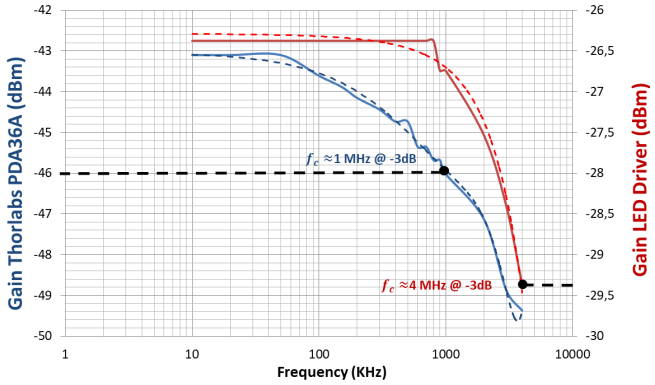

Fig. 4: Frequency response of the LED driver when connected to seven PC-LEDs at 100 mA of DC-bias current. Red lines: Electrical response (i_led vs. v_in). Blue lines: Optical response (v_pd vs. v_in). Solid lines: Measured values. Dashed lines: Polynomial approx. Cut-off freq. at 3 dB are shown for electrical and optical responses.

thermal voltage at a room temperature of 300 K, and I_s is the reverse current of the LED.

The DC constant signal model of an LED consists of a series resistance R_s and a diffusion capacitance C_d, which take different values according to the forward DC-bias conditions that are set. In order to determine these values, some of the parameters of the Shockley equation are needed to match the voltage and current pairs that are measured from the LED electrical response. In order to determine the emission coefficient N and the the reverse current I_s of the LED model under analysis, we use curve fitting methods to minimize the Mean Square Error (MSE) between measured $(V_\mathrm{led}, I_\mathrm{led})$ pairs with the ones predicted in (1). For further information about the details of this process, please refer to [13].

On the other hand, in order to study the AC response of the LED at different electrical frequencies, the small-signal model should be considered instead. For this purpose, the diffusion capacitance C_d and resistance r_d of the LED should be determined, such that the measured frequency response in the electrical domain can be accurately matched to the one approximated by the equivalent circuit in Fig. 3 b).

To carry out the practical validation of VLC-based monitoring system using ARQ signaling, an *ad hoc* LED driver (or VLC transmitter front-end) was designed and implemented to interface the voltage signal that comes from the USRP to the current that modulates the intensity of the light emitted by the PC-LEDs. The LED driver was designed to maximize the excursion of the output AC signal at different DC-bias levels, maximizing as much as possible the bandwidth of the input signal (*i.e.*, the cutoff frequency at 3 dB). The LED driver was based on a high-power MOSFET transistor, and included a pre-emphasis circuit that aimed at compensating the strong attenuation that the high-frequency components of the data-carrying signal experience due to the low-pass response of the Yellow-phosphor layer of the PC-LED. Fig. 4 shows the electrical response of the LED driver (red lines), as well as the optical response (blue lines) that includes the low-pass response of the yellow phosphor (measured at the PD output).

III. VLC-BASED MONITORING USING ARQ SIGNALING

When compared to RF communications, VLC systems suffer from more notable line-of-sight blockage when an obstacle (such as a person) is placed between the transmitter and receiver. According to the pace that this person takes when moving across the VLC services area, different ARQ signaling profiles will be generated. In this section, we first give the details of the ARQ scheme that was implemented. After that, we present the geometry of the sensing problem that was considered, which justifies the nature of the ARQ statistics that were collected when a person performed different activities.

A. Principles of Stop-and-Wait ARQ

Though different types of ARQ can be found in the literature, the most popular ones are the *Stop-and-Wait* ARQ, the *Go-Back-N* ARQ, and *Selective Repeat* ARQ. In this paper we focus on the Stop-and-Wait scheme, the most basic form of an ARQ protocol, which transmits one data block at a time and waits until a positive (ACK) or negative (NACK) confirmation of the reception of the data packet is signaled to the transmitter.

When the ARQ signaling is received by the transmitter, there are three possible scenarios: (a) The frame was successfully received with no errors (ACK), so the transmitter can send the following data block; (b) The data block that was received had errors (NACK), so the transmitter must re-send the same data block that was hold in a buffer, aiming at having better luck in the new attempt; (c) The data packet is never detected at the intended receiver and, due to that, the (N)ACK is never issued. To solve this latter problem, the Stop-and-Wait ARQ scheme implements a waiting time period known as *time-out*, giving enough time to receive the (N)ACK signaling under normal working conditions. If the (N)ACK confirmation is not received before the time-out timer expires, the data block is considered lost and a re-transmission process is triggered.

We note that in presence of normal working conditions, where no obstacle is placed between the VLC transmitter and receiver, ACKs are mainly received. However, in presence of a

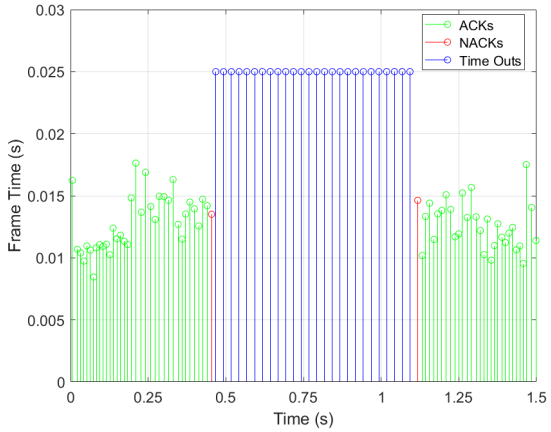

Fig. 5: Time-to-ACK for different data frames when the VLC link implements the Stop-and-Wait ARQ. ACKs are plotted in green dashed-dotted lines, whereas NACKs and time-outs are shown with red dotted and blue continuous lines, respectively.

partial VLC link blockage, the SINR of the received signal is reduced, and NACKs start to appear according the probability of bit error that the VLC link has. Finally, in case of full-blockage, the preamble of the VLC frame cannot be detected and, due to that, no (N)ACKs are issued by the receiver; in this situation, the time-out timer of the transmitter expires continuously until the VLC link can be recovered. This effect can be visualized in the central part of Fig. 5, where blue lines show the presence of time-out events during the whole duration of the full-blockage event in the VLC channel.

B. Geometry of the Indoor Monitoring based on ARQ

As previously stated, communication systems based on light suffer from blockage in presence of obstacles between the transmitter and the receiver. This fact causes deep fading events that impact the transmitted VLC signal, making difficult its detection at the receiver side. Though this phenomenon is a well-known downside of VLC, it can actually be considered as an advantage if the aim is to monitor the status of a point-to-point link. More precisely, it allows to measure variations in the (N)ACKS and time-outs of ARQ to determine if: i) A single person or multiple people created the obstruction; ii) The person waked in a given direction (or the opposite one) when it blocked the VLC link; iii) The person was walking or running when it obstructed the link. Toward this regard, the scenario for the VLC-based monitoring demonstration consists of an indirect communication link from a LED to a PD through a wall (see Fig. 6). The LED and PD are rotated an angle $\theta_{\rm led}$ and $\theta_{\rm pd}$, respectively, and are both separated from the wall at a distance of y, and between them at a distance x. The LED has an aperture radiation angle Ψ that concentrates the light from the LED inside the light spot that is projected on the wall. On the other hand, the reflection of the light from the wall to the PD is diffuse in nature and, due to that, the reflection angle of each light ray that hits the wall does not match with its incident angle. This effect makes the size of the second beam (*i.e.*, from the wall to the PD) much wider than the first beam (*i.e.* from the LED to the wall). To determine the blocking

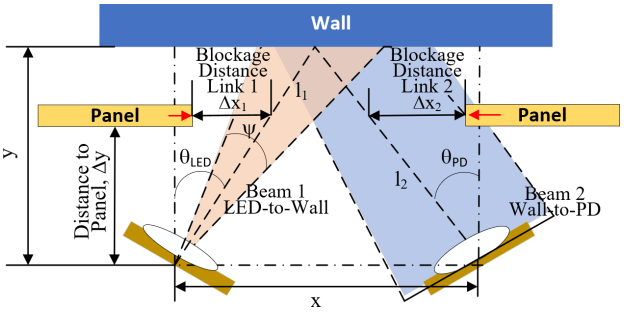

Fig. 6: VLC link geometry for ARQ indoor monitoring. $\theta_{\rm led}$ and $\theta_{\rm pd}$ represent the rotation angles of the LED and PD respectively, whereas Ψ is the aperture emission angle at half-power of the LED.

region of these two beams, denoted as $\Delta x_{\rm k}$, we have moved a panel from outside the two light beams towards their center, until the VLC receiver does not detect any transmitted data. Thus, denoting the time-out duration as $T_{\rm out}$ and the average speed at which the k-th light beam becomes blocked as $v_{\rm k}$, then the expected number of time-outs for beam k becomes

$$N_{\rm T_{out},k} = \Delta x_{\rm k}/(T_{\rm out} \times v_{\rm k}), \qquad \zeta = N_{\rm T_{out},2}/N_{\rm T_{out},1} \quad (2)$$

where $k = 1$ ($k = 2$) for the LED-to-wall (wall-to-PD) beam and ζ is the number of time-out ratio for both beams.

We note that the larger is the value that ζ takes, the more chances we have to estimate accurately the direction of the movement, the number of persons that obstruct the link, and the speed at which the person moves (walking or running) in the given test scenario (see Fig. 6). Unfortunately, when $\zeta \approx 1$, the number of time-outs when blocking each of the beams is similar, and it becomes very difficult to infer any conclusions by observing the statistics of the ARQ signaling. On the contrary, when $\zeta \gg 1$, it enables us to infer reliably the kind of activity that the person performed when blocking the VLC link. The value of ζ depends on several parameters, such as the distance of the blocking panel to the LED and PD, the speed at which the object moved when obstructing both beams, the emission angle at half-power of the LED, and the Field-of-View of the PD that varies if a concentrator lens is utilized. As a result, the number of time-outs has been modeled as a random variable, which can be characterized by a Probability Density Function (PDF) known as $f(x)$. Then, the conditional probabilities of the number of time-outs becomes

$$p(N_{\rm T_{out}}|N_{\rm T_{out},k}) = f(N_{\rm T_{out},k}, \mathbf{\Phi}) \quad (3)$$

where $\mathbf{\Phi}$ is a parameters that define the number of time-outs for beam k. Then, if $d_{N_{T_{out}}}$ identifies the decision threshold of the number of time-outs of the two beams, then the error probability in choosing the wall-to-PD beam (beam #2) instead of the beam between LED-to-wall (beam #1) becomes

$$p(b_2|N_{\rm T_{out}} = N_{\rm T_{out},1}) = \int_{d_{\rm N_{Tout}}}^{\infty} p(N_{\rm T_{out}}|N_{\rm T_{out},1})\, dN_{T_{out}}, \quad (4)$$

assuming that the number of time-outs in the wall-to-PD beam is much larger than the corresponding ones for the LED-

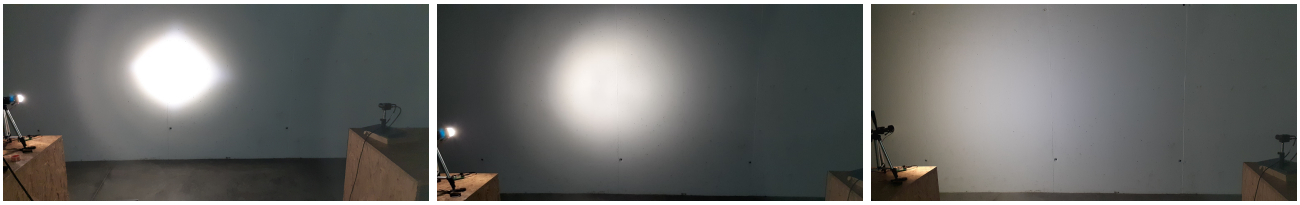

(a) LED emission angle $\Psi = 12$ deg. (b) LED emission angle $\Psi = 50$ deg. (c) LED emission angle $\Psi = 120$ deg.

Fig. 7: Illuminated spot that the light beam emitted by the LED projects over the white wall for different emission angles at half-power (Ψ).

TABLE I: Parameters of the VLC experimentation scenario and numerology of the single-carrier M-PAM frame that was implemented in the VLC link.

Symbol	VLC Link Parameter	Value	Unit
$d_{\text{led-wall}}$	Distance LED to wall	1	m
$d_{\text{wall-pd}}$	Distance wall to Photodetector	1	m
$d_{\text{led-pd}}$	Distance between LED and Photodetector	2.5	m
f_{s}	USRP sampling rate	1×10^6	Sa/s
T_{F}	Frame duration	0.576	ms
T_{out}	Time-out duration	25	ms

TABLE II: Blockage distance to the centers of LED-to-wall and wall-to-PD beams, including their ratio for different separations ($\Psi = 50$ deg.)

Distance Panel, Δy	Blockage Distance LED-to-wall beam, Δx_1	Blockage Distance wall-to-PD beam, Δx_2	Ratio, ζ
28.5 cm	6.2 cm	15.5 cm	2.5
38.5 cm	9 cm	24.5 cm	2.72
48.5 cm	10.5 cm	33 cm	3.14
58.5 cm	11.5 cm	35 cm	3.04

to-wall beam. Similarly, the error probability for inferring a blockage in beam #1 instead of in beam #2 is given by

$$p(b_1|N_{\text{T}_{\text{out}}} = N_{\text{T}_{\text{out}},2}) = \int_0^{d_{N_{\text{T}_{\text{out}}}}} p(N_{\text{T}_{\text{out}}}|N_{\text{T}_{\text{out}},2}) dN_{\text{T}_{\text{out}}}. \quad (5)$$

After introducing the theoretical background of our VLC-based monitoring concept, we are ready to explain our results.

IV. Experimental Results

This section summarizes the practical results that were obtained. Firstly, the experimental settings are explained and, after that, the performance analysis of obtained results is done.

A. Experimental setting

Table I summarizes the space and temporal metrics that were used to implement the VLC system for indoor monitoring. The rotation angle of the LED and PD were set to $\theta_{\text{led}} = 60$ deg. and $\theta_{\text{pd}} = 45$ deg., respectively. Concerning the emission angles of the LEDs, three different values $\Psi = 12$, 50, and 120 deg. were considered (the light spot projected on the wall in each case is shown in Fig. 7). However, only the results obtained for $\Psi = 50$ deg. are presented in detail in this paper since, for this configuration, the blockage distances from the center of the LED-to-wall and wall-to-PD beams are notably different. Toward this regard, Table II shows these blockage distance when the panel is separated at $\Delta y = 28.5$, 38.5, 48.5, and 58.5 cm from the LED and PD (see section III-B). Note that the larger is the separation from the blocking panel to the LED/PD (*i.e.*, Δy), the greater is the blockage distance Δx. Furthermore, the blockage distance of the wall-to-PD beam is much larger that the corresponding one for the LED-to-wall beam. As a result, if the velocity of the blocking object does not vary notably, it is possible to infer with high probability the activity that was carried out from the number of time-outs and/or (N)ACKs generated by the ARQ scheme.

After introducing the settings, next section shows the most relevant performance results when using the ARQ monitoring.

B. Performance analysis

This section shows the results obtained when using the ARQ signaling of a VLC link for activity monitoring. Specifically, the possibility to infer the following activities was considered from the received ARQ signalling pattern: i) When a person obstructs the LED-to-wall and wall-to-PD beams walking (see monitoring scheme showed in Fig. 6); ii) When a person blocks these two beams running; iii) When a (disabled) person using crutches walks in front of the VLC links (i.e., Healthcare use case); iv) When two people crosses the two light beams. The feedback channel was assumed reliable (*e.g.*, based on a robust radio wireless link); due to that, in these tests, the transmitter and receiver USRPs were connected with a wire.

Towards this regard, Fig. 8 shows their corresponding time-to-ACK. From there, it is possible to distinguish the four activities from the collected ARQ signaling. If a person walks, then the duration of the time-to-ACK augments with respect to the running case, as shown in Fig. 8 a) and 8 b). Note that when a (disabled) person with crutches or when two people walking obstruct the VLC link, the time-to-ACK increases even more than before, as shown in Fig. 8 c) and Fig. 8 d). However, the pattern of their time-to-ACK is different, since the speed of a person that walks with crutches tends to be more irregular than the one from two people without mobility problems.

Fig. 9 shows the Cumulative Distribution Function (CDF) of the number of time-outs (N_{to}) and NACKs (N_{nacks}) when a person obstructs the LED-to-wall and wall-to-PD beams walking. From the curves presented in this figure, it is possible to obtain several conclusions. Firstly, that the number of time-outs that is expected when blocking the LED-to-wall beam is lower than the ones that would correspond when blocking the wall-to-PD beam. In contrast, when measuring the number of NACKs, the opposite effect takes place. The reason for this behavior is that the size of the blocking region of the LED-to-wall beam is much smaller than the one of the wall-to-PD beam (see Table II). Consequently, it is expected that the dom-

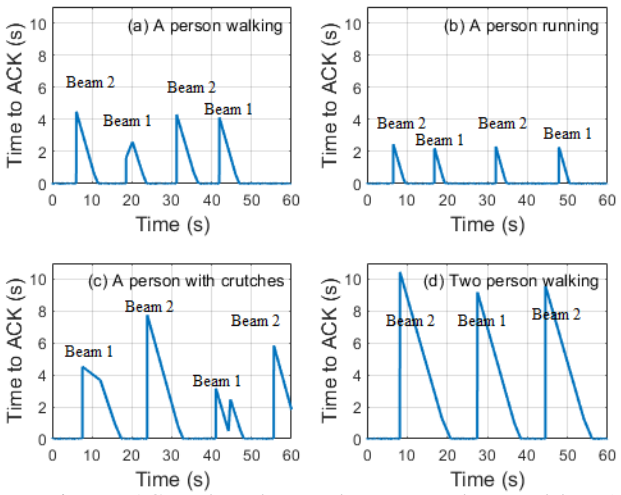

Fig. 8: Time-to-ACK when the two beams are obstructed by: a) A person walking; b) A person running; c) A person walking with crutches; d) Two people walking.

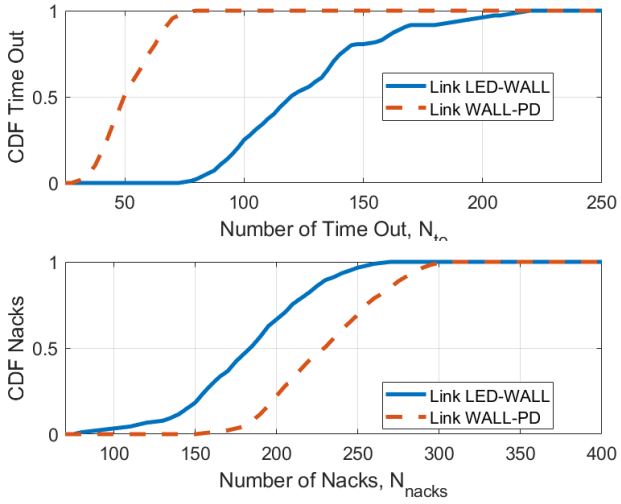

Fig. 9: CDF for the time-outs and NACKs that corresponds to the LED-to-wall beam (upper panel) and wall-to-PD beam (lower panel).

inant blockage event for the first beam will be a *full-blockage* whereas, in the second beam, the dominant event will be most likely a *partial-blockage*. In practice, this means that in case of *full-blockage*, the VLC receiver cannot detect the preamble sequence. Then, the transmitter does not obtain any feedback from the VLC receiver and, due to that, the time-out timer is activated. On the contrary, in presence of *partial-blockage*, the receiver is able to detect the preamble. However, the attenuation that the received VLC signal experiences is high enough to make some errors when detecting the received symbols. In this case, the VLC receiver sends a NACK to inform the transmitter that the frame was incorrectly received. In both cases the frames are re-transmitted but the trigger of ARQ re-transmissions is different. These ARQ patterns can be also used to determine the direction of the movement/activity.

Another interesting result is that the distance between the CDFs of the number of time-outs for the two links is much larger than their corresponding CDF for the number of NACKs. This means that there will be less error probability in classifying measuring the number of time-outs.

V. Conclusion

This paper studied the effect that different people's activities have on the ARQ signaling of VLC transmissions. The geometry of the scenario was based on an indirect communication setting, where the LED reaches the PD by reflecting its light on a large wall. As a result, the dominant blockage effect that experimented both LED-to-wall and wall-to-LED beam were different. In the LED-to-wall beam, the dominant blockage event was *full-blockage*, whereas in wall-to-PD beam, the most relevant event was the *partial-blockage*. Thus, the concept for which the frames are re-transmitted is different. By doing so, it is possible to detect if the person walk or run, and even if the person uses crutches or not. Future research lines will introduce machine learning algorithms to improve the classification of the different activities. That means measure the ARQ signaling during a predetermined temporal window size of suitable length, and apply a Machine Learning classifier to infer the activity with passive VLC-based monitoring.

References

[1] W. Jiang, B. Han, M. Habibi, and H. Schotten, "The road towards 6G: A comprehensive survey," *IEEE Open J. Commun. Society*, vol. 2, pp. 334–366, Feb. 2021.

[2] D. Karunatilaka, F. Zafar, V. Kalavally, and R. Parthiban, "LED based indoor visible light communications: State of the Art," *IEEE Commun. Surv. & Tut.*, vol. 17, no. 3, pp. 1649–1678, 3Q 2015.

[3] A. Dowhuszko, M. Ilter, and J. Hämäläinen, "Visible light communication system in presence of indirect lighting and illumination constraints," in *Proc. IEEE Int. Conf. Commun.*, June 2020, pp. 1–6.

[4] ——, "Visible light communications for indoor monitoring (VLADIMIR)," *Public deliverable of ATTRACT final conference*, pp. 1–5, Sept. 2020, [Online]. Available: https://attract-eu.com/wp-content/uploads/2019/05/VLADIMIR.pdf.

[5] F. Zafari, A. Gkelias, and K. Leung, "A survey of indoor localization systems and technologies," *IEEE Commun. Surv. Tut.*, vol. 21, no. 3, pp. 2568–2599, Apr. 2019.

[6] S. Yousefi, H. Narui, S. Dayal, S. Ermon, and S. Valaee, "A survey on behavior recognition using WiFi channel state information," *IEEE Commun. Mag.*, vol. 55, no. 10, pp. 98–104, Oct. 2017.

[7] M. Ilter, A. Dowhuszko, K. Vangapattu, K. Kutlu, and J. Hämäläinen, "Random forest learning method to identify different objects using channel estimations from VLC link," in *Proc. IEEE Int. Symp. Personal, Indoor and Mobile Radio Commun.*, Sept. 2020, pp. 1–6.

[8] R. Cam and C. Leung, "Throughput analysis of some ARQ protocols in the presence of feedback errors," *IEEE Trans. Commun.*, vol. 45, no. 1, pp. 35–44, Jan. 1997.

[9] S. Lindner, J. D. Kroening, P. N. Tran, C. Petersen, and A. Timm-Giel, "Analytic study of packet delay from 4G and 5G system ARQs using signal flow graphs," in *Proc. IEEE Veh. Tech. Conf.*, May 2020, pp. 1–5.

[10] A. Dowhuszko, M. Ilter, P. Pinho, R. Wichman, and J. Hämäläinen, "Effect of the color temperature of LED lighting on the sensing ability of visible light communications," in *Proc. IEEE Int. Conf. Commun. Workshops*, June 2021, pp. 1–6.

[11] Lumileds, "LUXEON Rebel — General purpose white," Apr. 2016, DS64 LUXEON Rebel General Purpose Product Datasheet, [Online]. Available: https://www.lumileds.com/wp-content/uploads/files/DS64.pdf.

[12] Thorlabs, "PDA100A2 Si switchable gain detector – User guide," May 2019, [Online]. Available: https://www.thorlabs.com/drawings/e10b5a31b41beb6f-17B4555E-A230-2E4C-BB120B00C3A97F91/PDA100A2-Manual.pdf.

[13] E. F. Schubert, *Light-Emitting Diodes*, 2nd ed. Cambridge University Press, 2006.